Computational phase diagrams of noble gas hydrates under pressure

Computational phase diagrams of noble gas hydrates under pressure

Pattanasak Teeratchanan and Andreas Hermann

Citation: The Journal of Chemical Physics **143**, 154507 (2015); doi: 10.1063/1.4933371
View online: http://dx.doi.org/10.1063/1.4933371
View Table of Contents: http://scitation.aip.org/content/aip/journal/jcp/143/15?ver=pdfcov
Published by the AIP Publishing

Computational phase diagrams of noble gas hydrates under pressure

Pattanasak Teeratchanan[a)] and Andreas Hermann[b)]
Centre for Science at Extreme Conditions and SUPA, School of Physics and Astronomy, The University of Edinburgh, Edinburgh EH9 3FD, United Kingdom

(Received 30 June 2015; accepted 6 October 2015; published online 21 October 2015)

We present results from a first-principles study on the stability of noble gas-water compounds in the pressure range 0-100 kbar. Filled-ice structures based on the host water networks ice-I_h, ice-I_c, ice-II, and C_0 interacting with guest species He, Ne, and Ar are investigated, using density functional theory (DFT) with four different exchange-correlation functionals that include dispersion effects to various degrees: the non-local density-based optPBE-van der Waals (vdW) and rPW86-vdW2 functionals, the semi-empirical D2 atom pair correction, and the semi-local PBE functional. In the He-water system, the sequence of stable phases closely matches that seen in the hydrogen hydrates, a guest species of comparable size. In the Ne-water system, we predict a novel hydrate structure based on the C_0 water network to be stable or at least competitive at relatively low pressure. In the Ar-water system, as expected, no filled-ice phases are stable; however, a partially occupied Ar-C_0 hydrate structure is metastable with respect to the constituents. The ability of the different DFT functionals to describe the weak host-guest interactions is analysed and compared to coupled cluster results on gas phase systems. © *2015 AIP Publishing LLC.* [http://dx.doi.org/10.1063/1.4933371]

I. INTRODUCTION

Clathrate hydrates are formed by water ice "host" structures that encapsulate some small and usually weakly interacting "guest" gases, be they atoms or molecules. The host water network is usually unstable by itself at ambient conditions because of the presence of sizeable cavities in the structures. However, the balance between energetic driving forces towards a fully hydrogen-bonded water network and the weak van der Waals-type interaction between host and guest helps stabilizing the clathrate structures, usually at modest pressures in the kbar range. Extensive studies from both experimental and theoretical groups on clathrate hydrates suggest that small-molecule guest gases like hydrogen, nitrogen, oxygen, methane, ammonia, etc., as well as inert noble gases can be enclosed in the host clathrate network.[1] As a result of their encapsulating capabilities, clathrate hydrates are important for our understanding of gas-water molecular compounds in icy comets and planets, have potential applications as gas transportation and storage materials, e.g., hydrogen storage, and play a role in climate evolution, as the melting of gas-hydrate such as methane can release a potent greenhouse gas.[2]

Known water clathrate structures include clathrate structure I (CS-I), clathrate structure II (CS-II), CS-H, and CS-T.[3] The first two are cubic structures, whereas the latter two have hexagonal and tetragonal unit cells, respectively. CS-I, space group $Pm\bar{3}n$, has 46 water molecules and eight cages (of two different sizes) per unit cell. CS-II, space group $Fd\bar{3}m$, has 136 water molecules and 24 cages (two sizes); CS-H, space group $P6/mmm$, has 52 water molecules and six cages (three sizes); and CS-T, space group $P4_2/mnm$, has 12 water molecules that form two cages.[4] The potential uptake of guests in any of these clathrates can vary as, depending on guest size, different cages can be occupied by less or more than one guest species. Alternatively, instead of inducing the formation of specific host networks, small guest species can also aggregate in the natural cavities present in water ice phases. These "filled ice" structures have been observed for hydrogen, helium, and neon hydrates, for instance.[4]

Here, we investigate the hydrates of the noble gases He, Ne, and Ar. These have been studied in the past to varying degrees. The only well characterised helium hydrate is based on the filled ice-II structure and found at pressures between 0.28–0.48 GPa.[5,6] There, the water:helium ratio is 6:1 at full occupancy (i.e., one He per cavity). Differential thermal analysis (DTA) by Dyadin *et al.*[7] found thermal anomalies in the 0.1-0.2 GPa range, suggesting the presence of a different phase at lower pressure. Molecular dynamics simulation by Malekov and Zheligovskaya[8] showed that occupying the cages in ice-II with one He atom each diminished the amplitude of molecular center of mass oscillation, thus leading to the stability of the helium inclusion compound. Recent *in situ* neutron diffraction by Yu *et al.* has shown the existence of neon hydrate at 0.48 GPa and 70-260 K.[9] Molecular dynamics studies confirmed the neutron diffraction result at 0.48 GPa and 260 K. These findings are in good agreement with results by Dyadin *et al.*[7] proposing from DTA measurements that neon may form an ice-II-based hydrate between 0.2-0.3 GPa. Three phases of argon hydrate are known to exist. At low pressure, argon forms a clathrate structure (ArH-I) based on CS-II. Neutron powder diffraction[10] experiments showed that ArH-I transforms to ArH-II, which adopts the CS-H structure, at 0.46 GPa. Then, at 0.77 GPa, ArH-II transforms to ArH-III, which adopts the CS-T framework.[11] Hirai *et al.*[12,13] performed

a)s1270872@sms.ed.ac.uk
b)a.hermann@ed.ac.uk

X-ray diffraction measurements and suggested a new phase at 1.1 GPa that is based on filled-ice-I_h structures.

A computational study on the phase diagrams of the noble gas hydrate system will contribute to our understanding, e.g., why some selective host water networks are suitable for particular hydrates. For example, helium hydrate forms based on filled ice-II but presumably not in any of the clathrate hydrate structures. The opposite is the case in argon hydrate, which can be found only in clathrate host frameworks but not in any "filled ice" structures.

The noble gases serve as prototypes for other guest molecules: helium and neon (atomic size 0.62 Å and 0.76 Å, respectively) model the H_2 molecule (d_{HH} = 0.74 Å); argon (atomic size 1.42 Å) substitutes for the O_2 or N_2 molecules (d_{OO} = 1.46 Å, d_{NN} = 1.50 Å). Therefore, we include the currently known phases of the hydrogen hydrates as templates for our calculations of the noble gas hydrates. At present, four structures of hydrogen hydrate have been determined experimentally under applied pressures, namely (ranging from low to high pressure), CS-II, C_0, C_1, and C_2. The CS-II hydrogen clathrate adopts the conventional clathrate hydrate CS-II structure[14,15] in the pressure range of 0.18-0.22 GPa, when cooled to around 200-250 K. This phase contains around 64 hydrogen molecules and 136 water molecules in the unit cell, which means a water:hydrogen ratio of approximately 2:1.[15] At 0.5 GPa, the C_0 clathrate, which does not adopt any of the known clathrate hydrates or filled-ice structures, was found to be stable with a water:hydrogen ratio of 2:1.[16,17] At higher pressure, the C_1 and C_2 phases form between 0.36-0.9 GPa, and around 2.4 GPa, respectively.[18,19] Both of these two phases adopt filled-ice structures. The C_1 phase has a 6:1 water:hydrogen ratio and is a filled-ice structure based on the hexagonal ice-II host framework, whereas the C_2 phase has a 1:1 ratio of water to hydrogen with the water host framework related to cubic ice-I_c.[18] Experimental work indicates a transformation from cubic C_2 to a tetragonal phase at higher pressure (around 10-20 GPa) and then a transformation to another phase at 45 GPa.[20,21] Recent density functional theory (DFT) predictions suggest a new phase called C_3, which is also based on cubic ice-I_c, to become stable at 38 GPa.[22] The C_3 phase accommodates the guest hydrogen molecules differently than the C_2 phase, which results in a water:hydrogen ratio of 1:2, the highest hydrogen storage content suggested so far. The same authors also suggest a new phase, which is based on filled ice-I_h, to compete with the proposed C_0 phase at low pressures.

Therefore, our choices of water host networks are ice-I_h, ice-I_c, ice-II, and C_0. The experimental structures of ferroelectric ice-XI ($Cmc2_1$) and its proposed metastable antiferroelectric analogue ($Pna2_1$) are chosen to represent the proton-disordered phase of ice-Ih. The C_0 network structure is based on the hexagonal ice framework suggested by Efimchenko *et al.*[16] (overall space group $P3_2$). While not fully resolved experimentally, several theoretical papers have established reasonable structural models for the oxygen network of the C_0 structure.[22,23] Accordingly, the network forms helically twisted channels running along the *c* axis that can be occupied by guest species. The channels are bulged such that they form a sequence of distinct cavities with canonical guest sites at their centres; the full occupation of which will result in a water:guest ratio of 2:1.

II. METHODOLOGY

Structural relaxations were performed by using DFT[24,25] with the Perdew-Burke-Ernzerhof (PBE) exchange-correlation functional[26] and several others (see below) and the projector augmented wave (PAW) method[27,28] to describe the electron-ion interaction, as implemented in the VASP code (version 5.3.3).[29] The plane wave cutoff energy (E_c = 875 eV) and Monkhorst-Pack k-point meshes[30] (density 20/Å^{-1}) were chosen to be large enough to fully converge total energies. The "hard" PAW data sets, with atomic cutoff radii (H = 0.80 a_0, O = 1.10 a_0, He = 1.10 a_0, Ne = 1.70 a_0, Ar = 1.90 a_0) were used in the calculations. Dispersion corrections of long-range electronic correlation effects were included along side the standard PBE functional to establish how they affected geometries, enthalpies, and stabilities of various phases. Two dispersion methods were used in this study, the semi-empirical van der Waals (vdW)-D2[31] and the electron density-based vdW-DF approach.[32,33] vdW-D2 is a correction to the total energy based on a pair-wise atomic interaction potential using tabulated parameters. The vdW-DF proposed by Dion *et al.* is a non-local dispersion functional dependent on the electron density. There are several varieties of the vdW-DF functionals. Here, we used both the optPBE-vdW[33] and the rPW86-vdW2[34] functionals. Structural relaxations with all functionals were performed until the net forces on each atom were smaller than 2 meV/Å.

III. RESULTS

A. Dispersion effects

Long range dispersion interactions, such as vdW forces, are crucial to predict relatively accurately the lattice energies and phase transition pressures between different molecular ice phases.[35,36] This has been seen, for instance, by accurate calculations of electron correlation energies in solid ice.[37] In the present work, we thus consider the results from four different exchange-correlation functionals: PBE, PBE+D2, optPBE+vdW, and rPW86-vdW2. Amongst these, the non-local density-based rPW86-vdW2 functional is assumed to provide the most accurate results. This was concluded from the work by Santra *et al.* on the importance of dispersion corrections for ice, comparing a series of vdW correction methods[36] (see also the supplementary material[38]). While water ice is now seemingly well understood, it is less clear which (if any) dispersion correction method would be most suitable to describe the inclusion compounds of the type of hydrates studied here; presumably, due to the nature of the weak interaction between host and guest, dispersion interactions will make a quantitative difference with regards to phase stabilities and transition pressures. However, since water is a polar molecule, the leading interaction is of the nature permanent dipole-induced dipole; much of these essential electrostatic interactions should be included in semi-local exchange-correlation functionals already. We therefore compare the

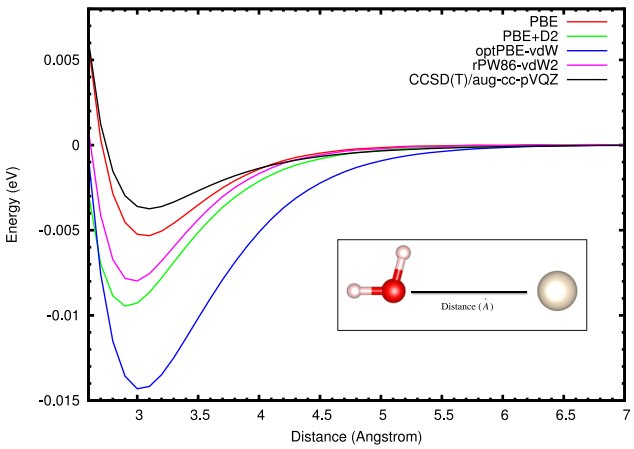

FIG. 1. Potential energy surface of the He–H_2O dimer interaction (geometry shown in inset), comparing various density- and wave function-based approaches, as function of the He–O separation.

non-local rPW86-vdW2 and optPBE-vdW methods with the semi-empirical PBE+D2 and the semi-local PBE functionals.

Initially, we investigated the interaction between a noble gas atom and an isolated water molecule, using various orientations of the latter. DFT results using VASP are compared to results from second-order Møller-Plesset perturbation theory (MP2) and coupled-cluster calculations (at the CCSD(T) level) using Gaussian,[39] where the latter will provide the most accurate estimate of the actual interaction energy. Augmented quadruple-zeta correlation consistent basis sets were used in those calculations.[40,41] The results of the He–H_2O interaction from different computational methods are shown in Figure 1 and tabulated in Table I. It is clear that all DFT methods overestimate the interaction considerably when compared to the CCSD(T) results. This is in agreement with other theoretical studies that find an overestimation of rare gas dimer binding energies using (semi-)local exchange-correlation functionals,[42] an issue that gets aggravated with additional explicit inclusion of long-range attractive interactions. While the PBE binding energy (amongst the small set of DFT methods used here) deviates least from the CCSD(T) result, all dispersion-corrected functionals overbind significantly, with the rPW86-vdW2 functional as closest approximant overestimating the dimer binding energy by more than a factor of two.

However, these issues do not necessarily translate into the description of the condensed state. Delocalisation of the electron density and screening effects could lead to a much better density functional-based description of solid hydrate phases than of the gas phase dimer. Such many-body effects have been studied recently for a methane-water cluster and rare gas-water trimers.[43,44] There, density functional methods were seen to feature significant three-body terms, which tend to cancel errors in the two-body (pair-wise) interactions in large molecular agglomerates. To estimate the relevant many-body effects here, we calculated the binding energy of a He atom inside a $(H_2O)_{12}$ cage taken out of the ice-II crystal structure. At MP2/aug-cc-pVDZ level of theory (using the Gaussian program), the binding energy is −22.1 meV (the larger aug-cc-pVQZ basis set might reduce this energy by about 25%, see the supplementary material[38]); using DFT with the rPW86-vdW2 functional, it is −24.9 meV—still slightly overbinding, but much less so than the He–H_2O dimer calculations would suggest.

Benchmarks of density functionals against diffusion Monte Carlo calculations for solid methane hydrate found that the accurate description of pure ice phases (the main ingredient in all hydrate phases) is crucial to obtain accurate hydrate cohesive energies.[45] Hence, while none of the DFT methods seem perfect to describe the noble gas hydrate compounds, we focus from here on the rPW86-vdW2 results as most meaningful. As $d_{O–He}$ is obtained quite accurately with this functional, we expect it to give accurate geometries of the hydrates, while some overbinding could mean an artificial stabilisation of hydrate phases compared to the elemental constituents.

TABLE I. Noble gas-water dimer interactions from various methods. For each noble gas, equilibrium distance $d_{O–NG}$ in Å and binding energy E_0 in meV are given.

Methods	He	Ne	Ar
MP2	(3.16, −2.88)	(3.18, −7.34)	(3.36, −17.28)
CCSD(T)	(3.10, −3.74)	(3.09, −9.01)	(3.37, −16.83)
PBE	(3.06, −5.38)	(3.21, −7.15)	(3.64, −8.65)
PBE+D2	(2.90, −9.54)	(3.02, −16.31)	(3.37, −21.18)
optPBE-vdW	(3.03, −14.39)	(3.13, −22.38)	(3.48, −31.03)
rPW86-vdW2	(2.99, −7.99)	(3.06, −14.28)	(3.38, −23.62)

B. He–H_2O compound system

Using ground state total energy calculations, we explored all possible phases in the He–H_2O system. As mentioned above, due to the similarity in size of He and H_2, the known phases of the H_2–H_2O system (with H_2 molecules replaced by He atoms) were used here, in addition to the only known He hydrate structure, filled ice-II. The relative enthalpies of formation of the various compounds are calculated with respect to pure ice phases and solid helium: $\Delta H_f(\mathrm{He}_n(\mathrm{H_2O})_m) = (H_f(\mathrm{He}_n(\mathrm{H_2O})_m) - n \cdot H_f(\mathrm{He}) - m \cdot H_f(\mathrm{H_2O}))/(n+m)$. Here, we restrict ourselves to ground state calculations: $H_f \approx F = E + pV$. We then construct the convex hull of all He–H_2O compounds by plotting ΔH_f versus the helium atomic content $x_{He} = n/(n+m)$; all points on the convex hull of such a plot are stable against all decomposition reactions. For all others, decomposition into various unary or binary phases is energetically favorable. The convex hull plot at $P = 1$ kbar is shown in Figure 2. The green tie-line is plotted to connect the points of the stable phases on the convex hull. At this pressure, we find He–H_2O compounds based on ice-II (C_1) and ice-I_h to be energetically favorable phases. In both stable phases, the obvious cavities in the host networks are fully filled. That leads to an overall H_2O:He ratio of 6:1 in filled ice-II, and 2:1 in filled ice-I_h. Note that the relative enthalpies of partially filled ice-II are not far removed from the convex hull. This means that a variety of ice-II based hydrates with varying degree of He occupancy may be formed experimentally, depending only on the He reservoir (i.e., its chemical potential) and potential diffusion barriers for He through the ice-II network. We also looked into over-filled ice-II (having two He atoms in one cavity), which

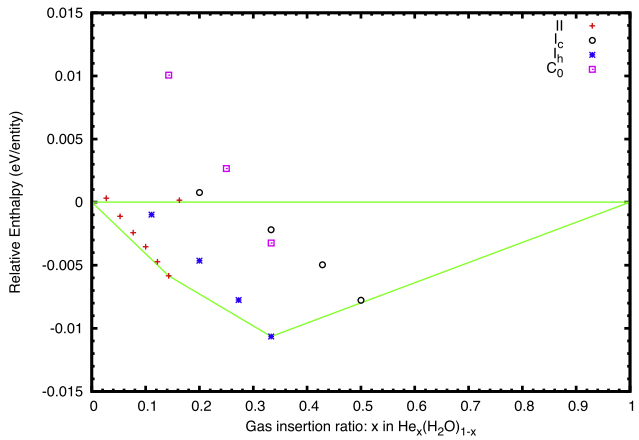

FIG. 2. Relative ground state enthalpies of formation for He–H_2O phases at P = 1 kbar, on the rPW86-vdW2 level of theory.

resulted in a large increase in enthalpy (see single red symbol at x_{He} = 0.167 in Figure 2). In contrast, partially filled ice-I_h structures are less favorable, and an enthalpic trend towards formation of fully filled ice-I_h hydrate is evident in Figure 2. The other water networks included in this study, C_0 and ice-I_c, did not form any stable helium hydrates at this particular pressure.

The fully filled ice-I_h hydrate is stable up to P = 5.26 kbar and the stability range of the fully filled ice-II phase is P = 0.36–18.9 kbar. One can already see in Figure 2, that a hydrate based on ice-I_c with H_2O:He = 1:1 is not far off stability. Indeed, we find this phase to become stable at slightly higher pressures, in the range P = 1.13–33.3 kbar. In hydrogen hydrate terminology, this is the C_2 hydrate phase: one He atom occupies each cavity in the ice-I_c water network. We do not find the predicted hydrogen hydrate C_3 phase, which is also based on the ice-I_c water network with H_2O:He = 1:2, to become stable up to P = 100 kbar. In that phase, the He atoms would be positioned not in the center of the cavities, but in the center of the water six-rings that form the boundary of each cavity.

We summarize the stability fields of the various He-hydrate phases in the left column of Figure 3. There, each thick solid line represents the pressure range where we find the respective phase to be stable. We also include, in thinner solid lines, metastable phases, where metastability is defined as being less than 1 meV/entity removed from stability. These phases include the partially filled ice-II and ice-I_h networks. Note that the different functionals give qualitatively very similar results, with respect to which phases are stable and their ordering as function of pressure. However, significant quantitative differences can be observed, for instance, PBE predicting a stable filled ice-II hydrate almost up to P = 70 kbar, and both PBE and optPBE-vdW predicting a stable C_3 hydrate above P = 80–90 kbar. Many of these differences can be traced back to the descriptions of the pure ice phases (the ice phase sequences are indicated in the phase diagrams in Figure 3). Overall, we find the phase sequence of helium hydrates to be very similar to that of the hydrogen hydrates; as could probably be expected due to the similarities in guest sizes and their interactions with the water host network.

C. Ne–H_2 O compound system

Using the same set of host ice structures, we computed the phase diagram of the Ne–H_2O system up to P = 100 kbar as well. We found a phase sequence of filled ice-I_h, filled ice-II (C_1), and filled ice-I_c (C_2) with increased pressure, expanding on the only experimentally known structure based on filled ice-II.[9] Note that we again adopt the H_2 hydrate convention for the phase notations in this context. Figure 4 shows the convex hull plot at P = 1 bar obtained using the rPW86-vdW2 functional. The only stable phases at P = 1 atm are based on fully filled ice-II (C_1) (shown as red plus symbol) and ice-I_h (shown as blue symbol). A structure based on filled C_0 (shown as purple square) is quasi-degenerate with the ice-I_h phase, with the energy difference around 2 meV/entity at P = 1 bar. Both C_0 and filled ice-I_h contain the same amount of Ne (H_2O:Ne = 2:1). That a neon hydrate based on the C_0 water network is energetically competitive with a filled ice-I_h structure is surprising and could warrant an experimental re-examination of the low-p/low-T phase diagram of Ne-H_2O. Note that in the otherwise quite similar He–H_2O system, the C_0 water network is significantly less stable. The structure based on filled ice-I_h remains stable up to P = 6.18 kbar, while the filled ice-II (C_1) phase with H_2O:Ne = 6:1 is stable in the pressure range from P = 1 atm to 23.6 kbar. We summarize the sequence of phase stabilities in the right column of Figure 3. Although a hydrate based on ice-I_c with H_2O:Ne = 1:1 (C_2) is unstable at low pressures, it becomes stable at P = 2.86 kbar and remains as such up to the highest pressure studied, P = 100 kbar. Structures with partially- and overly filled host cavities were also investigated. Apart from the filled ice-II phase, their relative enthalpies are less competitive than the stoichiometrically occupied phases.

Not unexpected, the series of stable phases in the Ne–H_2O system is calculated to be quite similar to the hydrogen and helium hydrates. This is likely due to the similar guest species sizes in these three compounds. Notably, we found the C_0 structure to be close to stability at very low pressures (about 2 meV/entity higher than filled ice-I_h). Using any of the other density functionals, the C_0 phase is predicted to have an actual range of stability before being superseded by filled ice-I_h as pressure is increased. The relative stability of the C_0 and ice-I_h hydrates is the only qualitative difference between the functionals, which otherwise give exactly the same hydrate sequence as function of pressure (with quantitative differences seen already for the He hydrates above). The phase with the highest guest content, based on filled ice-I_c with a H_2O:Ne ratio of 1:2 (C_3) was not stable in the pressure range studied here. Nonetheless, the C_0 may be kinetically stabilised over the ice-I_h phase, and the C_3 phase may become stable at higher pressures. In Figure 4 we also include metastable phases with enthalpies less than 1 meV/entity higher than the stable structures. The only thus-defined metastable phases in the Ne–H_2O compound system are based on partially filled ice-II.

D. Ar–H_2 O compound system

Ar–H_2O compounds based on the filled-ice water host networks studied here are not supposed to be stable—and

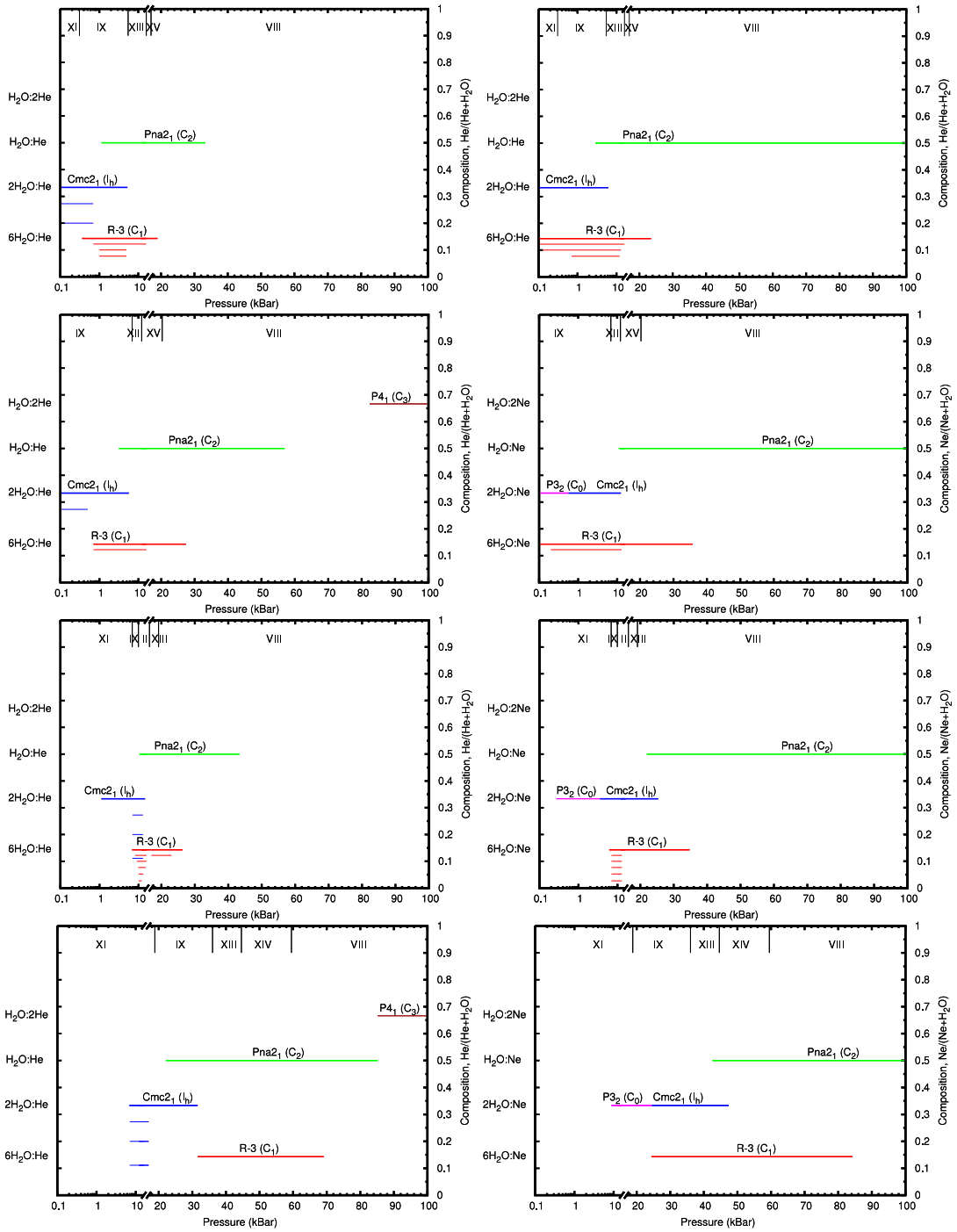

FIG. 3. Stability ranges of He-water (left) and Ne-water (right) ground state phases as function of pressure, as obtained from (top to bottom): the rPW86-vdW2, optPBE-vdW, PBE+D2, and PBE exchange-correlation energy functionals, respectively. Thick lines indicate stable phases, thin line metastable phases (see text). The ordinate axis sorts hydrates by chemical composition, and each stable phase is labelled by space group and H_2 hydrate notation, if applicable. Each plot shows at the upper edge the stability ranges of pure ice phases obtained from each functional.

we find this to be the case, with one exception: of all water host networks, only a partially filled C_0 compound is stable with respect to the elements. A cavity occupancy of 2/3 (i.e., a Ar:H_2O ratio of 1:3) leads to a relative enthalpy of formation of 3 meV/entity at P = 1 kbar—admittedly a very small stabilisation but maybe synthesisable as a metastable phase. Different functionals give slightly larger binding energies: 3.6 and 4.8 meV/entity for PBE+D2 and PBE, at P = 10 and 20 kbar, respectively. The structure of the partially filled C_0 network is shown in Figure 5. We compare this metastable phase to the traditional clathrate structure I (CS-I, with Ar:H_2O = 0.148) and structure II (CS-II, with Ar:H_2O = 0.15): both are found to be much more stable, with relative enthalpies of formation of 12 and 11 meV/entity at P = 1 kbar, respectively. Nevertheless, from both Ne and Ar hydrates a trend emerges: that the C_0 network is positioned between the filled-ice and the classical clathrate phases, in terms of the sizes of guest species it can take up.

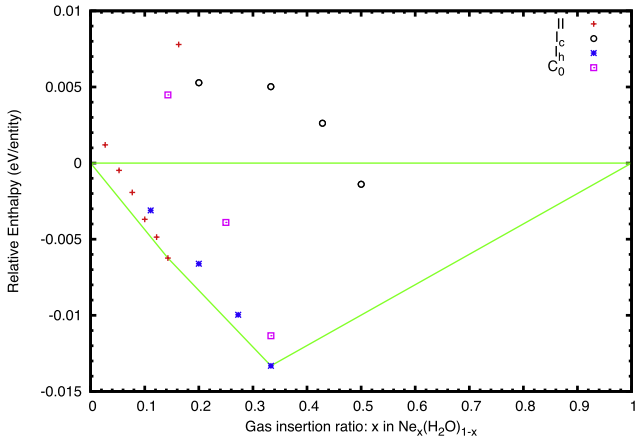

FIG. 4. Relative ground state enthalpies of formation for Ne–H_2O phases at $P = 1$ atm, on rPW86-vdW2 level of theory. The compound based on fully filled C_0 has a slightly higher relative enthalpy than the structure based on filled ice I_h.

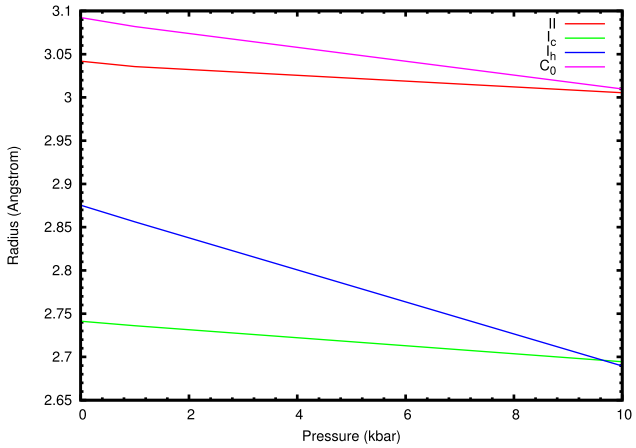

FIG. 6. Pressure evolution of cavity sizes of different host water networks from P = 1 atm to 10 kbar.

IV. DISCUSSION

A. Cavity size vs host network stability

The discussion on the relationship between cage sizes in clathrates and guest size was initiated by von Stackelberg and updated by Sloan.[1,46] The very intuitive argument is that guest species of a particular size "fit" or do not "fit" the cages provided by the classical clathrate water networks. Can similar conclusions be drawn for the filled-ice structures, and can the sequence of stable hydrates, e.g., seen in He or Ne hydrates, be rationalized by the pressure evolution of the cavity sizes in the water networks? We measured these cavity sizes as the diameters of the largest spheres to be inscribed into the water host structures without touching any of the host network nuclei. The results, obtained from calculations with the rPW86-vdW2 functional over a range of pressures (Figure 6), show that the ambient pressure stable ices I_h and I_c have smaller cavities throughout than the high-pressure phase ice-II and that the C_0 network has the largest cavities (see also Figure 7). All filled ices have much smaller cavities (between 2.74 and 3.04 Å) than the classical clathrate networks—clathrate structure CS-II, for example, has a cage size of 4.7 Å.

Correlating the predicted structural sequence of the noble gas hydrates to the evolution of cavity sizes in their host networks does, however, prove difficult. For He hydrates, for example, the sequence $I_h \rightarrow II \rightarrow I_c$ hardly follows a trend that could be related to Figure 6. It seems instead that, not surprisingly, the hydrates' host networks correlate to the most stable ice phase in a particular pressure regime (these stability ranges, as calculated from the different functionals, are indicated in Figure 3). Comparing different guest species, however, a familiar trend emerges: larger guests favour, under comparable conditions, networks with larger cavities; hence a predicted region of stability for a Ne–C_0 hydrate, and the only metastable filled-ice Ar hydrate, partially filled Ar–C_0.

B. Corrections to the host-guest interaction

The phase diagrams obtained from different first-principles descriptions (using the rPW86-vdW2, optPBE-vdW, PBE+D2, and PBE exchange-correlation functionals) produce qualitatively very similar results, as seen in Figure 3, for both He and Ne filled-ice hydrates: the same stable phases and transition sequences are predicted with all functionals. However, the predicted transition *pressures* and stability *ranges* of specific phases depend on the specific functional used. This is due to the different descriptions of the host-guest interactions by these functionals. For instance, as seen in Figure 1 and Table I, the optPBE-vdW functional provides accurate host-guest equilibrium separations, but tends to overestimate the interaction energy. This overbinding effect may shift the phase stabilities of hydrate phases towards lower pressures than seen experimentally. The calculations with nonlocal density-based dispersion corrections suggest the stabilities of some phases at pressures as low as P = 1 atm. The pairwise PBE+D2 correction suffers from combined effects of too-short equilibrium separations and overbinding of the host-guest interaction. While overbinding prefers to stabilize the hydrate mixtures at low pressures, a significant compression of the network structures is needed to benefit from the attractive part of the host-guest potential energy surface. As a result, the PBE+D2 calculations yield narrower regions of stability,

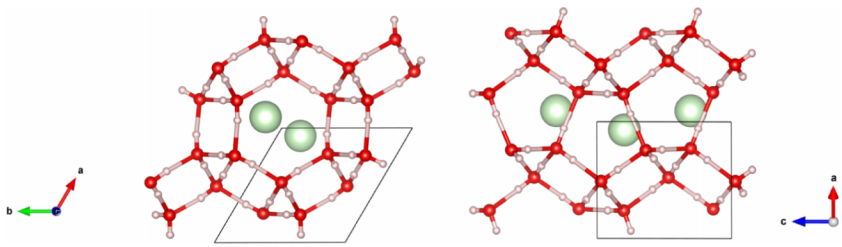

FIG. 5. Two views of the partially filled Ar–C_0 hydrate, along (left) and perpendicular to the channels in the C_0 network. Unit cell and hydrogen bonds in the water network are indicated.

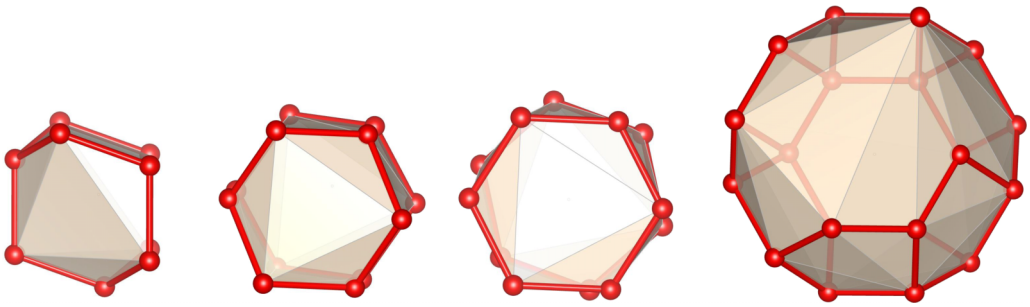

FIG. 7. Cavities of different host water networks, ranging from the smallest to the largest, and drawn to the same scale: ices I_c, I_h, II, and clathrate C_0. Protons are omitted.

which commence at higher pressures than in the rPW86-vdW2 calculations. In the case of PBE, the host-guest binding energy is slightly overestimated, while providing an almost correct equilibrium separation. However, PBE and other semilocal GGA functionals tend to overestimate the stability ranges of molecular ice networks by almost an order of magnitude (see Figure 3)[47] and are only appropriate to describe ice phases at much higher pressures.[48,49] It is then likely that the stability ranges of the gas hydrates are similarly overestimated. In fact, studies on the phase transitions of molecular ice phases using various functionals have shown that the rPW86-vdW2 functional provides very good agreement with experiment.[35,36] Therefore, we assume that the rPW86-vdW2 approach will be the most accurate method for comparing the relative enthalpies of systems comprising different water networks.

An *ad-hoc* correction is possible, using the quantum chemical potential energy surface of He–H_2O shown in Figure 1. We can correct the total energy of the hydrate phases by performing a many-body decomposition of the total energy into monomer and dimer terms; and replacing the guest-water dimer rPW86-vdW2 interaction energies with CCSD(T) values,

$$\Delta H_f(\mathrm{He_n(H_2O)_m}) = \Delta H_f^{\mathrm{DFT}}(\mathrm{He_n(H_2O)_m}) + \int dr\, g_O(r)(E_{PES}^{\mathrm{CCSD(T)}}(r) - E_{PES}^{\mathrm{DFT}}(r)). \quad (1)$$

Here, we correct the relative enthalpy of formation by subtracting the DFT overbinding and adding the CCSD(T) interaction energy for the host-guest interaction instead. The energies $E_{PES}(r)$ are shown in Figure 1, and weighted with the radial oxygen distribution $g_O(r)$ for each distance r from the guest atoms. Figure 8 illustrates the influence of the correction term: there, we show the guest-oxygen neighbour histogram, the difference between the DFT/rPW86-vdW2 and CCSD(T) dimer potential energy surfaces shown in Figure 1, and the resulting energy correction according to Eq. (1). We can see that the integrated DFT overbinding in the hydrate is estimated to be 40 meV per guest atom, and is dominated by the first water coordination shell, which makes up the cavity.

By supplanting the total energies from the rPW86-vdW2 functional with CCSD(T) results for the He–H_2O dimers for each phase and pressure, the convex hull plots (Figure 2 for He–H_2O and Figure 4 for Ne–H_2O) can be adjusted. The revised relative enthalpies of formation are compared to the original results in Figure 9 for He at P = 1 kbar and Figure 10 for Ne at P = 1 bar.

According to Figures 9 and 10, the crudely corrected enthalpies imply that most hydrate structures are unstable with respect to their constituents, bar for ice-II and C_0-based structures. As discussed previously, in Section III A, it is not clear whether DFT indeed overestimates the host-guest interaction in the condensed phase to the same extent as seen in the He/Ne–H_2O dimer. Results on the $He(H_2O)_{12}$ cluster indicate

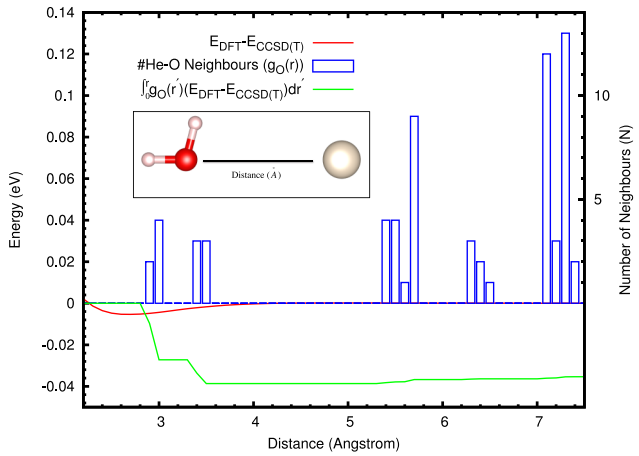

FIG. 8. He–H_2O in the filled ice-I_h framework: He–O neighbour histogram as bar plot; the difference between the DFT and CCSD(T) potential energy surface for the configuration shown in the inset; and the integrated energy correction.

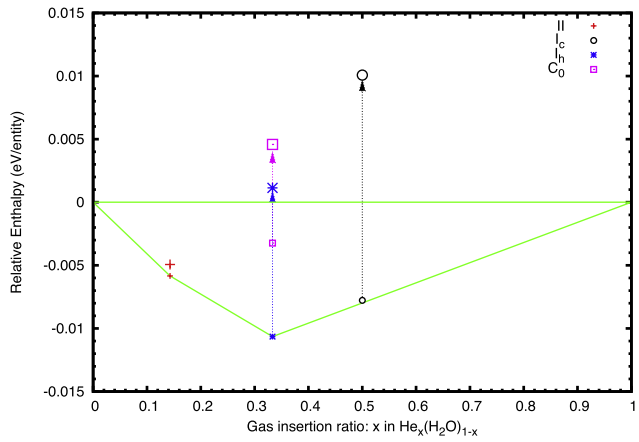

FIG. 9. Comparison of the relative ground state enthalpies of formation for fully filled He–H_2O phases at $P = 1$ kbar, showing results from rPW86-vdW2 (small symbols) and the corrected CCSD(T) values for the He–H_2O interaction (large symbols), respectively.

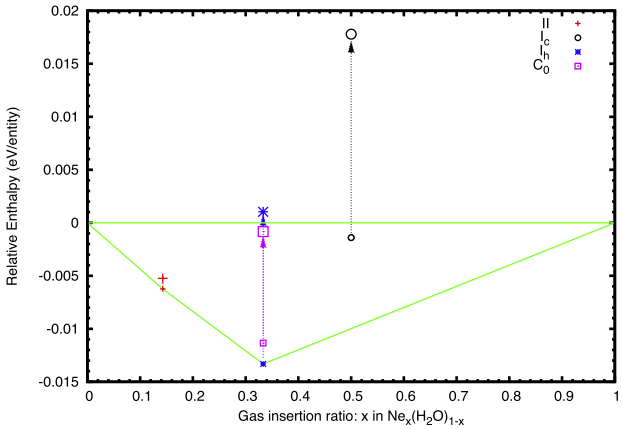

FIG. 10. Relative ground state enthalpies of formation for fully filled Ne–H_2O phases at $P = 1$ atm, showing results from rPW86-vdW2 (small symbols) and the corrected CCSD(T) values for the Ne–H_2O interaction (large symbols), respectively.

that DFT overbinding is much less pronounced in larger molecular agglomerates—whether that is due to error cancellation in DTF in different many-body terms[43] or the ability of the functionals to describe the pure ice phases very well[45]. The correction to the relative enthalpies of formation from Eq. (1) and Figures 9 and 10 should thus be seen as giving upper bounds for these hydrates.

The He/Ne–H_2O dimer interaction depends quite strongly on the relative orientation of the water molecule to the noble gas atom. In the supplementary material,[38] we show the potential energy surfaces for several He–H_2O configurations, amongst them the configuration used in Figure 1 and Eq. (1). Ultimately, using, for instance, the local-MP2 approach or a many-body decomposition of the total energy such as implemented in the method of increments would replace the simple energy correction of Eq. (1) in a more general and systematic manner and enable better judgement on the quality of density functional theory to describe these gas hydrates.[50–52]

We note that dispersion-corrected density functional theory overestimates the interaction between other closed-shell molecular species just as much. For instance, a correct description of hydrogen hydrates (of interest in hydrogen storage and for planetary science) requires an accurate treatment of the H_2–H_2O interaction; as shown in Figure 11, dispersion-corrected density functional theory overestimates the binding energy of the H_2–H_2O complex by up to a factor of four, while the semilocal PBE functional gives a surprisingly appropriate description of the potential energy surface.

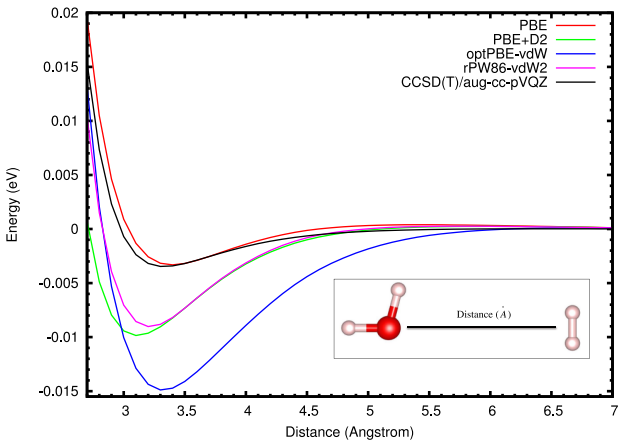

FIG. 11. Potential energy surface of the H_2–H_2O interaction as a function of H_2–O distance, comparing various density- and wave function-based approaches.

V. CONCLUSION

In summary, we present a comprehensive study of the ground state phase diagrams of noble gas-water compounds, based on first-principles calculations of various filled-ice structures. Our calculations determine stable phases for both the helium and neon compound systems based on four distinct host water networks, namely, ices I_h, II, and I_c, as well as the new water network C_0. The predicted sequence of stable helium-water compounds compares very well to the stable structures found in the hydrogen-water system: stable phases based on the host water networks of ice I_h, II, and I_c were found, in that order, upon increasing pressure. The recently discovered water network C_0 was found to form a stable (or at least competitive) Ne hydrate at very low pressure. The phase evolution of the Ne-water system is then a sequence of C_0/ice-I_h, ice-II, and ice-I_c host water networks, in that order, upon increasing pressure. Regarding possible filled-ice Ar-water mixtures, only one metastable structure was found, based on the C_0 host network, with partial occupancy of the guest sites. This phase is metastable with respect to the well-known CS-I and CS-II.

These results agreed qualitatively irrespective of the particular density functional used; however, quantitative differences with respect to predicted stability ranges of various phases exist. Moreover, all density functional methods used here tend to overestimate the interaction energy between the host and guest species, at least in small gas phase systems. While this overbinding might be less pronounced in the extended state, it could lead to an overestimation of the stability of the hydrate mixtures, as compared to the separated constituents. A simple correction of the pairwise host-guest interaction, using coupled cluster results for the dimer potential energy surface, should provide an upper bound for the hydrate binding energies; here, such a correction led to metastability of most considered hydrates structures. Specialized treatment of the weak host-guest interactions, for example, with local-MP2 or incremental methods, might be instructive and lead to further insight into these systems.

ACKNOWLEDGMENTS

P.T. would like to thank the Royal Thai Scholarship for graduate student support. Computational resources provided by the ARCHER UK National Supercomputing Service (Project ID d56) are gratefully acknowledged.

[1]J. E. D. Sloan, Nature **426**, 353 (2003).
[2]P. Englezos and J. Lee, Korean J. Chem. Eng. **22**, 671 (2005).
[3]A. Kurnosov *et al.*, Dokl. Phys. Chem. **381**, 303 (2001).
[4]J. Loveday and R. Nelmes, Phys. Chem. Chem. Phys. **10**, 937 (2008).
[5]D. Londono, J. Finney, and W. Kuhs, J. Chem. Phys. **97**, 547 (1992).
[6]D. Londono, W. Kuhs, and J. Finney, Nature **332**, 141 (1988).
[7]Y. Dyadin *et al.*, J. Struct. Chem. **40**, 790 (1999).

[8]G. Malenkov and E. Zheligovskaya, J. Inclusion Phenom. **48**, 45 (2004).
[9]X. Yu *et al.*, Proc. Natl. Acad. Sci. U. S. A. **111**, 10456 (2014).
[10]A. Manakov *et al.*, Dokl. Phys. Chem. **378**, 148 (2001).
[11]A. Manakov *et al.*, J. Inclusion Phenom. **48**, 11 (2004).
[12]H. Hirai *et al.*, Proc. Jpn. Acad., Ser. B: Phys. Biol. Sci. **78**, 39 (2002).
[13]H. Hirai *et al.*, J. Phys. Chem. B **106**, 11089 (2002).
[14]Y. Dyadin *et al.*, Mendeleev Commun. **9**, 209 (1999).
[15]W. Mao *et al.*, Science **297**, 2247 (2002).
[16]V. Efimchenko *et al.*, J. Alloys Compd. **509**, 860 (2011).
[17]T. Strobel, M. Somayazulu, and R. Hemley, J. Phys. Chem. C **115**, 4898 (2011).
[18]W. Vos *et al.*, Phys. Rev. Lett. **71**, 3150 (1993).
[19]V. Antonov, V. Efimchenko, and M. Tkacz, J. Phys. Chem. B **113**, 779 (2009).
[20]S. Machida *et al.*, J. Chem. Phys. **129**, 224505 (2008).
[21]H. Hirai *et al.*, J. Chem. Phys. **137**, 074505 (2012).
[22]G. Qian *et al.*, Sci. Rep. **4**, 5606 (2014).
[23]G. S. Smirnov and V. V. Stegailov, J. Phys. Chem. Lett. **4**, 3560 (2013).
[24]P. Hohenberg and W. Kohn, Phys. Rev. **136**, 864 (1964).
[25]W. Kohn and L. Sham, Phys. Rev. **140**, 1133 (1965).
[26]J. Perdew, K. Burke, and M. Ernzerhof, Phys. Rev. Lett. **77**, 3865 (1996).
[27]P. E. Blöchl, Phys. Rev. B **50**, 17953 (1994).
[28]G. Kresse and D. Joubert, Phys. Rev. B **59**, 1758 (1999).
[29]G. Kresse and J. Furthmüller, Phys. Rev. B **54**, 11170 (1996).
[30]H. Monkhorst and J. Pack, Phys. Rev. B **13**, 5188 (1976).
[31]S. Grimme, J. Comput. Chem. **27**, 1787 (2006).
[32]M. Dion *et al.*, Phys. Rev. Lett. **92**, 246401 (2004).
[33]J. Klimes, D. Bowler, and A. Michaelides, Phys. Rev. B **83**, 195131 (2011).
[34]K. Lee, E. D. Murray, L. Kong, B. I. Lundqvist, and D. C. Langreth, Phys. Rev. B **82**, 081101 (2010).
[35]B. Santra *et al.*, Phys. Rev. Lett. **107**, 185701 (2011).
[36]B. Santra *et al.*, J. Chem. Phys. **139**, 154702 (2013).
[37]A. Hermann and P. Schwerdtfeger, Phys. Rev. Lett. **101**, 183005 (2008).
[38]See supplementary material at http://dx.doi.org/10.1063/1.4933371 for crystallographic information on all relevant ice and hydrate phases, and phase sequences of pure ices computed with the different functionals.
[39]M. Frisch *et al.*, GAUSSIAN 09, Revision D.01, Gaussian, Inc., Wallingford, CT, 2009.
[40]J. T. H. Dunning, J. Chem. Phys. **90**, 1007 (1989).
[41]D. Woon and J. T. H. Dunning, J. Chem. Phys. **98**, 1358 (1993).
[42]T. van Mourik and R. Gdanitz, J. Chem. Phys. **116**, 9620 (2002).
[43]M. J. Gillan, J. Chem. Phys. **141**, 224106 (2014).
[44]M. J. Deible, O. Tuguldur, and K. D. Jordan, J. Phys. Chem. B **118**, 8257 (2014).
[45]S. J. Cox, M. D. Towler, D. Alfè, and A. Michaelides, J. Chem. Phys. **140**, 174703 (2014).
[46]M. von Stackelberg, Naturwissenschaften **36**, 327 (1949).
[47]A. Hermann and P. Schwerdtfeger, Phys. Rev. Lett. **106**, 187403 (2011).
[48]A. Hermann, N. W. Ashcroft, and R. Hoffmann, Proc. Natl. Acad. Sci. U. S. A. **109**, 745 (2012).
[49]A. Hermann, N. W. Ashcroft, and R. Hoffmann, Phys. Rev. B **88**, 214113 (2013).
[50]H. Stoll, J. Chem. Phys. **97**, 8449 (1992).
[51]C. Müller and B. Paulus, Phys. Chem. Chem. Phys. **14**, 7605 (2012).
[52]A. Erba *et al.*, J. Phys. Chem. B **113**, 2347 (2009).